Knee Surg Sports Traumatol Arthrosc (2010) 18:1679–1684
DOI 10.1007/s00167-010-1111-7

EXPERIMENTAL STUDY

The effect of microRNA-21 on proliferation and matrix synthesis of chondrocytes embedded in atelocollagen gel

Wirat Kongcharoensombat · Tomoyuki Nakasa · Masakazu Ishikawa · Atsuo Nakamae · Masataka Deie · Nobuo Adachi · Abouheif Mohamed · Mitsuo Ochi

Received: 17 September 2009 / Accepted: 3 March 2010 / Published online: 27 March 2010

Abstract The objective of this study was to investigate the effect of microRNA-21 (miR-21) on the proliferation and matrix synthesis of chondrocytes embedded in atelocollagen gel. Articular cartilage was harvested aseptically from the knee and hip joints of rats. In the experimental group, double-stranded miR-21 was transfected into the chondrocytes, and in the control group, scrambled siRNA was used. After that, chondrocytes were cultured in atelocollagen gel for 3 weeks. At 1, 2, and 3 weeks after transfection, the cell numbers were counted, and the expression levels of Col2a1 and aggrecan were measured by real-time PCR. Histological analysis by toluidine blue staining was performed at 3 weeks. The cell number in the experimental group rapidly increased compared to the control group. The expression levels of Col2a1 and aggrecan in the experimental group were higher than in the control. Histological analysis revealed that many more cells with a metachromatic stain were present in the experimental group than in the control. This study demonstrated that miR-21 promotes high proliferation and matrix synthesis of chondrocytes embedded in atelocollagen gel.

Keywords MicroRNA-21 · Chondrocytes · Atelocollagen gel · Three-dimensional culture · Gene expression

W. Kongcharoensombat (✉) · T. Nakasa · M. Ishikawa · A. Nakamae · M. Deie · N. Adachi · A. Mohamed · M. Ochi
Department of Orthopaedic Surgery, Programs for Applied Biomedicine, Division of Clinical Medical Science, Graduate School of Biomedical Sciences, Hiroshima University, Minami-ku, Hiroshima, Japan
e-mail: kwirat2003@yahoo.com

Introduction

These days, orthopaedic surgeons accept that it is difficult for articular cartilage lesions to self-repair, because of the limitations of the inflammatory and reparative response in articular cartilage. Moreover, chondrocytes surrounded by a rich extracellular matrix cannot migrate to the injury site [4]. So the treatment of full-thickness defects of articular cartilage remains a problem.

In 1994, a monolayer cultured system of autologous chondrocytes implantation (ACI) was reported [3]. But this injected chondrocytes technique may depend on the side of the defect, which occurs mainly as a result of gravity. In addition to this, chondrocytes are not distributed evenly in the space, which runs the risk of causing uneven cartilage regeneration after transplantation. Moreover, chondrocytes in monolayer culture dedifferentiate, thereby decreasing the gene expression level of type II collagen, while at the same time increasing the gene expression level of type I collagen. The technique of autologous chondrocyte implantation has been developed using a three-dimensional culture of chondrocytes [19]. However, the limited number of chondrocyte cells which can be harvested is one of the major problems. For promotional purposes, several studies which have combined additional techniques such as growth factors [8], hydrostatic pressure [16], dynamic compression [6], and gene therapy [12] have been conducted.

MicroRNAs (miRNAs) are small non-coding RNAs that target protein-coding mRNAs by repressing mRNA translation or causing its degradation [22]. MicroRNAs comprise about 22 nucleotides, derived from long-transcript pri-miRNAs and pre-miRNAs [2]. It is believed that there are as many as 1,000 miRNAs in the human genome and that up to 30% of human genes are regulated by miRNAs. For some human genes, more than one miRNA may be

involved in their regulation [10]. miRNAs play a crucial role in human diseases, and several therapeutic trials in vivo have been conducted. In orthopaedic fields, new tissue engineering combined with microRNA could lead to a novel regenerative treatment.

MicroRNA-21 (miR-21) is reported as being an important regulator of cell proliferation. Several studies have demonstrated that miR-21 plays a role in cancer. In this study, we evaluated the effect of microRNA-21 on the proliferation of chondrocytes embedded in atelocollagen gel. There have been no reports and no published literature about the effect of microRNA on chondrocytes until now.

Materials and methods

The animals were kept in the research facilities for laboratory animal science at Hiroshima University. The research protocol of this experiment was reviewed and approved by the university ethical committee.

Articular cartilage of 8-week-old male Sprague–Dawley rats was harvested from the bilateral femoral head and knee using the aseptic technique. Articular cartilage specimens were minced and washed in 0.9% sodium chloride. Chondrocytes were isolated by treatment with 0.25% trypsin (Gibco, CA, USA) in sterile saline for 30 min, followed by 0.25% collagenase type 2 (Gibco, CA, USA) in Dulbecco's modified Eagle's medium (DMEM,Gibco, CA, USA), supplemented with 10% fetal bovine serum (FBS) (Sigma, Taufkirchen,Germany), and antibiotics (penicillin [10,000 Units/ml], streptomycin [10,000 μg/ml] (Nacalai tesque, Japan) for 4 h at 37°C in a culture tube. The chondrocytes were washed three times with culture medium and then filtered through a sterile 70-mm nylon mesh (cell strainer, BD Biosciences Discovery Labware, Franklin Lakes, NJ, USA).

Atelocollagen/miRNA or siRNA complex was prepared according to the previous description [15]. An equal volume of atelocollagen (Koken, Tokyo, Japan) and miRNA or siRNA solution was combined and mixed by rotation at 4°C for 20 min. In the experimental group, 50 nM of double-stranded miR-21 (B-Bridge International, Inc. CA) was used, together with scrambled siRNA (siRNA negative control, B-Bridge International, Inc. CA). To examine the transfection efficiency, FAM-labeled double-stranded miRNA (Hokkaido System Science, Sapporo, Japan) was used. The complex was then kept at 4°C for 16 h before use. The final concentration of atelocollagen was 0.008%.

Isolated chondrocytes numbering 1.0×10^4 cells were dispersed and mixed in 100-μl atelocollagen gel. They were then put into 6-well culture plates and incubated in a mixture of 5% CO_2 and 95% air at 37°C for 30 min. Subsequently, atelocollagen complex with chondrocytes formed a gel. After that, a culture medium containing FBS and antibiotics was added into each well and incubated in a mixture of 5% CO_2 and 95% air at 37°C for 3 weeks. The culture medium was changed every 3 days, and L-ascorbic acid (50 μg/ml) was added every 2 days. At 24 h after starting incubation, fluorescent microscopic observation of FAM-labeled miRNA was performed to prove the high transfection efficiency. At 1, 2, and 3 weeks, the cell number, gene expression level, and histology were evaluated.

Regarding cell number, at postculture weeks 1, 2, and 3, atelocollagen gel was collected and then incubated with a solution containing 0.25% trypsin and 0.25% collagenase in DMEM at 37°C for 30 min to isolate the chondrocytes. The cell numbers were counted in a hemocytometer using the trypan blue dye exclusion test.

Synthesis of complementary DNA (cDNA) and Quantitative (real-time) PCR

At postculture weeks 1, 2, and 3, total RNA was isolated from the chondrocytes from atelocollagen gels that had been homogenized on ice with Trizol reagent (Invitrogen) for polymerase chain reaction (PCR) analysis. Total RNA yields were calculated, and the quality was determined using absorption spectrochemical analysis. One microgram of total RNA was reverse-transcribed using the Quanti-Tect® Reverse Transcription Kit (Qiagen, Chatsworth, CA) according to the manufacturer's protocol. The genomic DNA elimination reaction was carried out using 2 μl of gDNA wipeout buffer, 1 μg (1 μl) template RNA, and 11 μl RNase-free water at 42°C for 2 min. Reverse transcription was performed in 1 μl quantiscript reverse transcriptase, 4 μl quantiscript RT buffer, 1 μl RT primer mix, and 14 μl template RNA (the entire genomic DNA elimination reaction) at 42°C for 15 min and 95°C for 3 min, and then the cDNA product was maintained at 4°C.

Quantitative RT-PCR assays were performed using a TaqMan miRNA assay kit (Applied Biosystems, CA, USA) for mature miR-21 and SYBR Green (Applied Biosystems, CA, USA) for Col2a1 and aggrecan. Reverse transcriptase reactions of mature miRNAs contained a sample of the total RNA, 50 nM stem-loop RT primer, 10 × RT buffer, 100 mM each dNTPs, 50 U/μl MultiScribe reverse transcriptase, and 20 U/μl RNase inhibitor. Fifteen-microliter reactions were incubated in a thermocycler (BioRad, Hercules, CA) for 30 min at 16°, 30 min at 42°, 5 min at 85°, and held at 4°. Real-time PCR was performed using a Mini Opticon Real-time PCR System (BioRad, Hercules, CA) in a 10-μl PCR mixture containing 1.33 μl RT product, 2 × TaqMan Universal PCR Master Mix, 0.2 μM TaqMan probe, 15 μM forward primer, and 0.7 μM reverse primer.

Each SYBR Green reaction was performed with a 1.0 μl template cDNA, 10 μl SYBR Green mix, 1.5 μM primer, and water to adjust the final volume to 20 μl. Primer sequences were as follows: Col2a1, 5′-TCC TAA GGG TGC CAA TGG TGA-3′ (forward), 5′-AGG ACC AAC TTT GCC TTG AGG AC-3′ (reverse); aggrecan, 5′-CAC AGG CAG CAC AGA CAC TT-3′ (forward), 5′-CCC ACT TTC TAC AGG CAA GC-3′(reverse); β actin, 5′-GGA GAT TAC TGC CCT GGC TCC TA-3′ (forward), 5′-GAC TCA TCG TAC TCC TGC TTG CTG-3′ (reverse). All reactions were performed in triplicate, incubated in a 48-well plate at 95° for 10 min, followed by 40 cycles of 95° for 15 s, and 60° for 1 min. The snoRNA-135 or β actin gene was used as a control to normalize differences in total RNA levels in each sample. A threshold cycle (C_T) was observed in the exponential phase of amplification, and quantification of relative expression levels was performed using standard curves for target genes and the endogenous control. Geometric means were used to calculate the $\Delta\Delta C_T$ (delta-delta C_T) values and were expressed as $2^{-\Delta\Delta CT}$. The value of each control sample was set at 1 and used to calculate the fold-change of target genes.

In the third week of culture, the atelocollagen gels were collected, fixed in 4% paraformaldehyde solution, and then embedded in paraffin. Each paraffin-embedded sample was sectioned at 5 μm and stained with 0.1% toluidine blue for histological examination.

Statistical analysis

The data were analyzed using the Mann–Whitney *U*-test to determine significant differences between the two groups. A confidence level of 95% ($P < 0.05$) was chosen for statistical significance. Data are presented as mean value ± SD.

Results

To confirm the high transfection efficiency, fluorescence of FAM-labeled ds miRNA was observed. No fluorescence was observed in the atelocollagen gel using non-FAM-labeled scrambled siRNA (Fig. 1a). However, green fluorescence emission in the cells was well observed in the atelocollagen gel using FAM-labeled miRNA (Fig. 1b). Green fluorescence emission could be observed throughout the gel.

The number of chondrocytes in the atelocollagen gel in the experimental group was significantly higher at 1, 2, and 3 weeks than in the control group (Fig. 2). At 1 week, the chondrocytes in the experimental group proliferated ten-fold, while the chondrocytes in the control increased five-fold. The cell number in the experimental group rapidly increased for 3 weeks, whereas the chondrocytes in the control gradually increased. By the end of 3 weeks, the chondrocytes in the experimental group reached 30-fold.

To examine the expression level of cartilage-specific markers, Col2a1 and aggrecan, real-time PCR was performed. The expression level of Col2a1 and aggrecan in chondrocytes in the experimental group rapidly increased during the three weeks of culture. On the other hand, the chondrocytes in the control showed that Col2a1 and aggrecan expression slightly increased in the first week, then sustained in the second and third week (Fig. 3). Overexpression of miR-21 could effect the up-regulation of matrix synthesis via chondrocyte proliferation. The expression level of mature miR-21 was analyzed using real-time PCR. At 1 and 2 weeks, miR-21 in the experimental group significantly up-regulated, compared to that in the control (Fig. 4). These data indicated that overexpression of miR-21 could contribute to the up-regulation of Col2a1 and aggrecan via chondrocyte proliferation.

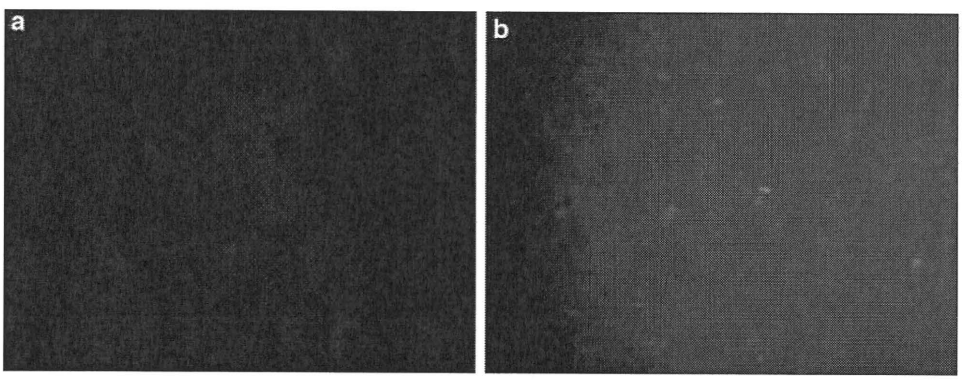

Fig. 1 Fluorescence observation to confirm the transfection efficiency. **a** Non-FAM-labeled scrambled siRNA was transfected. **b** FAM-labeled miRNA was transfected. Green fluorescence emission in the cells was well observed in the atelocollagen gel using FAM-labeled miRNA. Original magnification ×100

Histology sections with toluidine blue staining showed that many more cells with a metachromatic stain presented in the experimental group than in the control (Fig. 5).

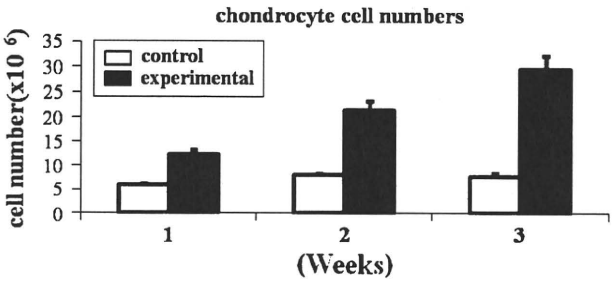

Fig. 2 This graph shows that the cell numbers of chondrocytes gradually increased in the experimental group, whereas the level plateaued in the control group

Discussion

The most important finding of the present study was that miRNA-21 promoted high proliferation and matrix synthesis of chondrocytes that are embedded in atelocollagen gel.

The discovery of RNA interference (RNAi) revealed a new mechanism for gene regulation, and the biochemical machinery involved plays a key role in many essential cellular processes [7]. After being discovered only a decade ago, several different types of RNAi now have been identified, such as siRNA and miRNA. Recently, the spotlight has been on miRNA, because they play a crucial role in human diseases. Many studies have tried to reveal this role by analyzing expression patterns or by examining how their function can lead to novel therapeutic methods. Several therapeutic trials on regulation of miRNAs in vivo were reported. Tazawa et al. reported that local injection of

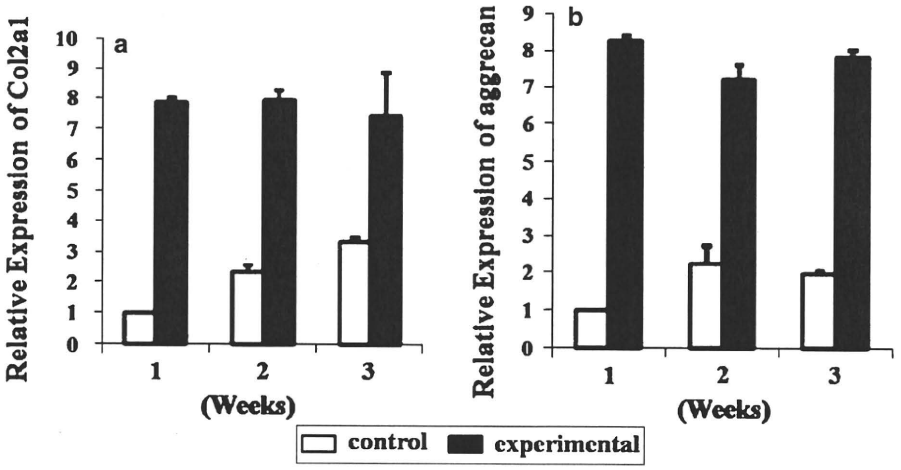

Fig. 3 The expression level of Col2a1 and aggrecan using real-time PCR. The expression level of Col2a1 and aggrecan in chondrocytes in the experimental group rapidly increased during the three weeks of culture. On the other hand, the chondrocytes in the control showed that Col2a1 and aggrecan expression slightly increased in the first week, then sustained in the second and third week

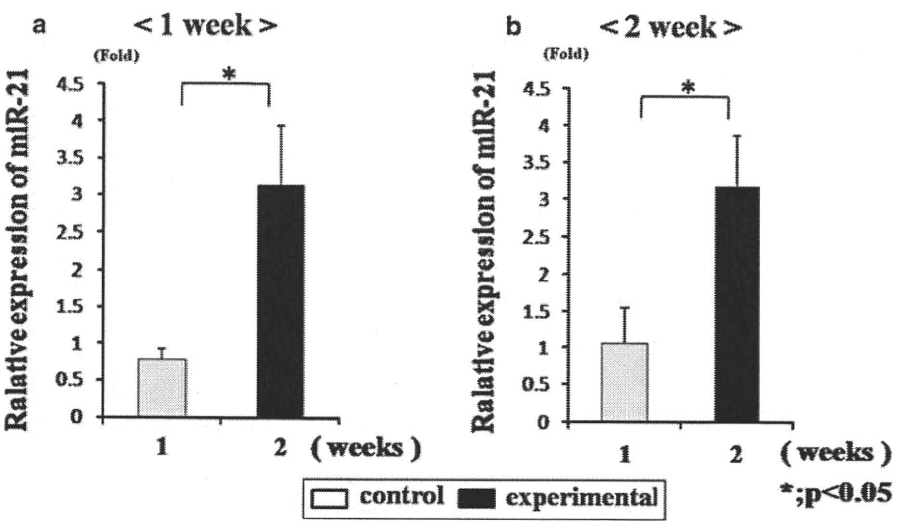

Fig. 4 The expression level of mature miR-21 using real-time PCR. At 1 and 2 weeks, miR-21 in the experimental group significantly up-regulated compared to that in the control

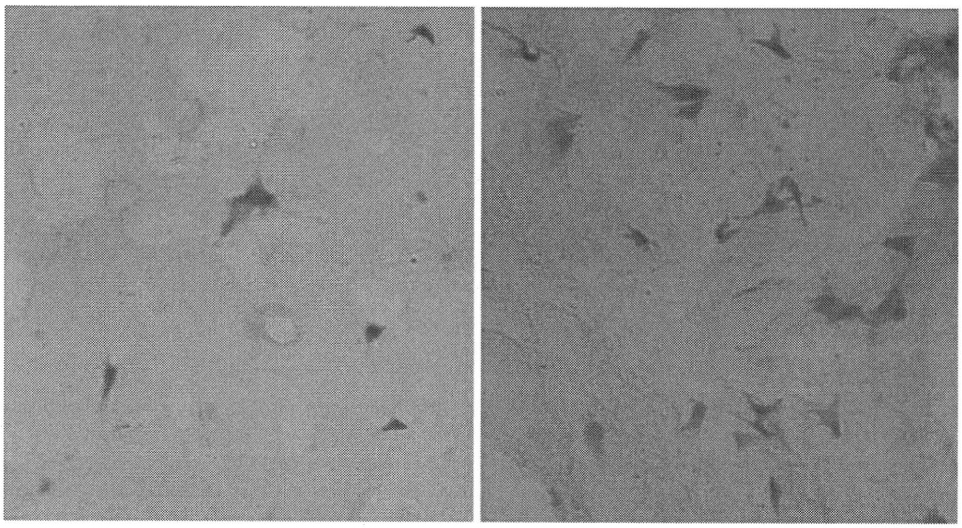

Fig. 5 Histological analysis using toluidine blue staining. Toluidine blue staining showed that many more cells with a metachromatic stain were present in the experimental group than in the control. Original magnification ×400

ds miR-34a complexed with atelocollagen could suppress the tumor growth in mice [21]. Nakasa et al. demonstrated that local injection of miR-1, miR-133, and miR-206 could promote the muscle regeneration in rat skeletal muscle injury model [17]. Nagata et al. reported that intra-articular injection of ds miR-15a could induce apoptosis in the synovium in arthritic mice [18]. New evidence for therapeutic application of miRNA was included. However, there are no reports on how the intervention of miRNA can modify tissue engineering.

This study, with its successful short-term results, has shown that ACI could lead to a breakthrough in cartilage repair [3]. However, there are some problems to solve. One problem is the limited number of chondrocytes which can be harvested from the unloaded area of the femoral condyle. Several studies have demonstrated the efficacy of cytokines or growth factors on cell proliferation and matrix synthesis [9, 13]. In this study, to solve the problem of the limited cell number obtained from normal cartilage, we tried to promote cell proliferation in atelocollagen by over-expression of miR-21. Atelocollagen used in the current study was for gene delivery such as siRNA [15]. High transfection efficiency was confirmed by FAM-labeled miRNA, as well as high expression of miR-21 could be maintained for 2 weeks by real-time PCR analyses. Indeed, over-expression of miR-21 could cause proliferation of the chondrocytes in the atelocollagen gel.

miR-21 is shown to target and down-regulate the expression of the tumor suppressors tropomyosin 1 [23], phosphatase and tensin homolog (PTEN) [14], promote cell invasion, metastasis, and programmed cell death 4 (Pdcd4) [1]. Its expression may be associated with TGFβ expression [20]. Knockdown of miR-21 in cultured glioblastoma cells triggers activation of caspases and leads to increased apoptotic cell death [5], while its over-expression inhibits apoptosis in myeloma cells [11]. According to the role of miR-21 on cell proliferation, we suspect that miRNA-21 can improve the proliferation of chondrocytes and the quality of extracellular matrix in vitro. These results suggest that modification of ACI by miRNAs might be one of the most promising methods of improving the quality of tissue-engineered cartilage.

However, this study had some limitations. First, atelocollagen gel being a three-dimensional structure posed some difficulty in the evaluation using FAM-labeled miRNA. Second, this was an in vitro study, striking a new area of research, so it was difficult to find similar studies in literatures to compare our results with, but we hope in future that this study opens the gate for new researches both in vitro and in vivo about the effect of miRNA on articular cartilage, paving the way for novel therapeutic intervention in the field of cartilage repair.

Conclusion

miRNA-21 promotes high proliferation and matrix synthesis of chondrocytes that are embedded in atelocollagen gel. Further studies are needed to confirm effective cartilage repair by implantation of tissue-engineered cartilage using our procedure in vivo.

Conflict of interest statement None of the authors have received any financial support from any organizations to influence this study.

References

1. Asangani IA, Rasheed SA, Nikolova DA, Leupold JH, Colburn NH, Post S, Allgayer H (2008) MicroRNA-21 (miR-21) post-transcriptionally downregulates tumor suppressor Pdcd4 and stimulates invasion, intravasation and metastasis in colorectal cancer. Oncogene 27:2128–2136
2. Bartel DP (2004) MicroRNAs: genomics, biogenesis, mechanism, and function. Cell 116:281–297
3. Brittberg M, Lindahl A, Nilsson A, Ohlsson C, Isaksson O, Peterson L (1994) Treatment of deep cartilage defects in the knee with autologous chondrocyte transplantation. N Engl J Med 331:889–895
4. Buckwalter JA, Mankin HJ (1998) Articular cartilage: tissue design and chondrocyte-matrix interactions. Instr Course Lect 47:477–486
5. Chan JA, Krichevsky AM, Kosik KS (2005) MicroRNA-21 is an antiapoptotic factor in human glioblastoma cells. Cancer Res 65:6029–6033
6. De Croos JN, Dhaliwal SS, Gryynpas MD, Pilliar RM, Kandal RA (2006) Cyclic compressive mechanical stimulation induces sequential catabolic and anabolic gene changes in chondrocytes resulting in increased extracellular matrix accumulation. Matrix Biol 25:323–331
7. Fire A, Xu S, Montgomery MK, Kostas SA, Driver SE, Mello CC (1998) Potent and specific genetic interference by double-stranded RNA in Caenorhabditis elegans. Nature 391:806–811
8. Iwasaki M, Nakata K, Nakahara H, Nakase T, Kimura T, Kimata K, Caplan AI, Ono K (1993) Transforming growth factor-beta 1 stimulates chondrogenesis and inhibits osteogenesis in high density culture of periosteum-derived cells. Endocrinology 132:1603–1608
9. Kawasaki K, Ochi M, Uchio Y, Adachi N, Matsusaki M (1999) Hyaluronic acid enhances proliferation and chondroitin sulfate synthesis in cultured chondrocytes embedded in collagen gels. J Cell Physiol 179:142–148
10. Lee RC, Feinbaum RL, Ambros V (1993) The *C. elegans* heterochronic gene lin-4 encodes small RNAs with antisense complementarity to lin-14. Cell 75:843–854
11. Loffler D, Brocke-Heidrich K, Pfeifer G, Stocsits C, Hackermuller J, Kretzschmar AK, Burger R, Gramatzki M, Blumert C, Bauer K, Cvijic H, Ullmann AK, Stadler PF, Horn F (2007) Interleukin-6 dependent survival of multiple myeloma cells involves the Stat3-mediated induction of microRNA-21 through a highly conserved enhancer. Blood 110:1330–1333
12. Madry H, Kaul G, Cucchiarini M, Stein U (2005) Enhanced repair of articular cartilage defects in vivo by transplanted chondrocytes overexpressing insulin-like growth factor I (IGF-I). Gene Ther 12:1171–1179
13. Matsusaki M, Ochi M, Uchio Y, Shu N, Kurioka H, Kawasaki K, Adachi N (1998) Effects of basic fibroblast growth factor on proliferation and phenotype expression of chondrocytes embedded in collagen gel. Gen Pharmacol 31:759–764
14. Meng F, Henson R, Weh-Janek H, Ghoshal K, Jacob S, Patel T (2007) MicroRNA-21 regulates expression of the PTEN tumor suppressor gene in human hepatocellular cancer. Gastroenterology 133:647–658
15. Minakuchi Y, Takeshita F, Kosaka N, Sasaki H, Yamamoto Y, Kouno M, Honma K, Nagahara S, Hanai K, Sano A, Kato T, Terada M, Ochiya T (2004) Atelocollagen-mediated synthetic small interfering RNA delivery for effective gene silencing in vitro and in vivo. Nucleic Acids Res 32:e109
16. Miyanishi K, Trindade MC, Lindsey DP, Beaupre GS, Carter DR, Goodman SB, Schurman DJ, Smith RL (2006) Dose- and time-dependent effects of cyclic hydrostatic pressure on transforming growth factor-beta3-induced chondrogenesis by adult human mesenchymal stem cells in vitro. Tissue Eng 12:2253–2262
17. Nakasa T, Ishikawa M, Shi Ming, Shibuya H, Adachi N, Ochi M (2009) Acceleration of muscle regeneration by local injection of muscle-specific microRNAs in rat skeletal muscle injury model. J Cell Mol Med in press. PMID: 19754672
18. Nagata Y, Nakasa T, Mochizuki Y, Ishikawa M, Miyaki S, Shibuya H, Yamasaki K, Adachi N, Asahara H, Ochi M (2009) Induction of apoptosis in the synovium of autoantibody-mediated arthritis in mice by the intra-articular injection of double-stranded microRNA-15a. Arthritis Rheum 60:2677–2683
19. Ochi M, Uchio Y, Tobita M, Kuriwaka M (2001) Current concepts in tissue engineering technique for repair of cartilage defect. Artif Organs 25:172–179
20. Qian B, Katsaros D, Lu L, Preti M, Durando A, Arisio R, Mu L, Yu H (2008) High miR-21 expression in breast cancer associated with poor disease-free survival in early stage disease and high TGF-beta1. Breast Cancer Res Treat 117:131–140
21. Tazawa H, Tsuchiya N, Izumiya M, Nakagama H (2007) Tumor-suppressive miR-34a induces senescence-like growth arrest through modulation of the E2F pathway in human colon cancer cells. Proc Natl Acad Sci USA 104:15472–15477
22. Zamore PD, Haley B (2005) Ribo-gnome: the big world of small RNAs. Science 309:1519–1524
23. Zhu S, Si ML, Wu H, Yin-Yuan M (2007) MicroRNA-21 targets the tumor suppressor gene tropomyosin 1 (TPM1). J Biol Chem 282:14328–14336

The Knee xxx (2010) xxx–xxx

Contents lists available at ScienceDirect

The Knee

Case Reports

Two cases of synovial haemangioma of the knee joint: Gd-enhanced image features on MRI and arthroscopic excision

Takahisa Sasho *, Koichi Nakagawa, Kei Matsuki, Hiroko Hoshi, Masahiko Saito, Naoshi Ikegawa, Ryuichiro Akagi, Satoshi Yamaguchi, Kazuhisa Takahashi

Dept. of Orthopaedic Surgery, Graduate School of Medicine, Chiba University, Chiba Japan

ARTICLE INFO

Article history:
Received 12 May 2010
Received in revised form 8 September 2010
Accepted 2 October 2010
Available online xxxx

Keywords:
MRI
Gadolinium
Haemangioma
Knee
Intraarticular lesion

ABSTRACT

Synovial haemangioma of the knee joint is a relatively rare benign condition with around 200 reported cases. We have recently encountered two cases of synovial haemangioma of the knee joint which preoperative MRI had assessed as highly suspect and which arthroscopic resection and subsequent histological examinations confirmed as synovial hemangiomas. Published studies have identified the following as characteristic MRI features of synovial haemangioma: homogenous low intensity to iso-intensity on T1 sequence; and heterogeneous high intensity with low-intensity septa or spots within the lesion on T2 sequence. However, several other intra-knee disorders mimic these characteristics. In our two cases, we found that gadolinium (Gd)-enhanced images, which have been relatively rarely discussed in the literature, were useful for making the diagnosis and for determining the extent of this condition. These images also were very helpful during arthroscopic excision of the lesion. Nonetheless, even after Gd enhancement, differentiating between malignant conditions such as synovial sarcoma and haemangioma solely from MRI findings is still difficult.

1. Introduction

Synovial haemangioma of the knee joint is a relatively rare, benign condition with around 200 cases reported in the English literature [1]. The advent of MRI has facilitated non-invasive diagnosis of this condition [2], but MRI studies alone cannot definitively establish the diagnosis of synovial haemangioma because a variety of intraarticular tumorous conditions, including malignancy, can have a similar MRI appearance. We recently have encountered two cases of synovial haemangioma of the knee joint which preoperative MRI had assessed as highly suspect and which arthroscopic resection and subsequent histological examinations confirmed as synovial hemangiomas. We observed that the Gd-enhanced MRI images were particularly useful for making the diagnosis and for determining the extent of this condition. Since few studies of synovial haemangioma in the literature have discussed Gd-enhanced MRI images [3–5], we have focused in this report on describing the Gd-enhanced MRI features of our two cases of synovial haemangioma and comparing these features with the Gd-enhanced MRI features of other tumorous conditions arose in the knee joint reported in the literature. Characteristic features of synovial haemangioma are also discussed.

2. Case 1

A 37 year-old woman had been suffering from continual right knee pain since she was 9 years old. She had episodes of haemarthrosis approximately once a year until she was age 15, but an arthroscopic examination at age 13 showed no intra-joint abnormalities. Despite the persistence of her knee pain over the next 22 years, she had no further occurrences of haemarthrosis after age 15 until she had an acute episode of haemarthrosis two months before referral to our hospital that brought her to an orthopaedic surgeon. This episode was followed by five additional episodes of haemarthrosis during a short period of time. X-ray examination and MRI detected an abnormal intraarticular mass (Fig. 1), resulting in her being referred to our hospital for diagnosis and treatment.

At our institution, we performed a Gd-enhanced MRI that clearly depicted the extent of her lesions (Fig. 2). An obscure region on T1 and T2 images (Fig. 1, #) was found out to be a satellite lesion. Her past history of haemarthrosis along with the MRI findings was indicative of haemangioma, and we performed arthroscopy for the confirmation of the diagnosis and treatment (Fig. 3, left). Gd-enhanced images were very helpful for the arthroscopic surgery because they guided us in making portals for arthroscopy at spra-patella pouch that would avoid direct penetration into the tumorous lesion. We totally excised the lesion until the patella tendon was totally exposed (Fig. 3, right) as planned preoperatively due to MRI findings, and histological examination confirmed that the lesion was a cavernous haemangioma. The patient experienced a substantial reduction in her pain soon after surgery and returned to her work as a nursery teacher two weeks after surgery. No sign of recurrence was observed 2 years after surgery.

* Corresponding author. Department of Orthopaedic Surgery, Graduate School of Medicine, Chiba University 1-8-1, Inohana, Chuo-ku, Chiba 260-8670, Japan. Tel.: +81 43 226 2117; fax: +81 43 226 2116.

0968-0160/$ – see front matter © 2010 Elsevier B.V. All rights reserved.
doi:10.1016/j.knee.2010.10.004

Please cite this article as: Sasho T, et al, Two cases of synovial haemangioma of the knee joint: Gd-enhanced image features on MRI and arthroscopic excision, Knee (2010), doi:10.1016/j.knee.2010.10.004

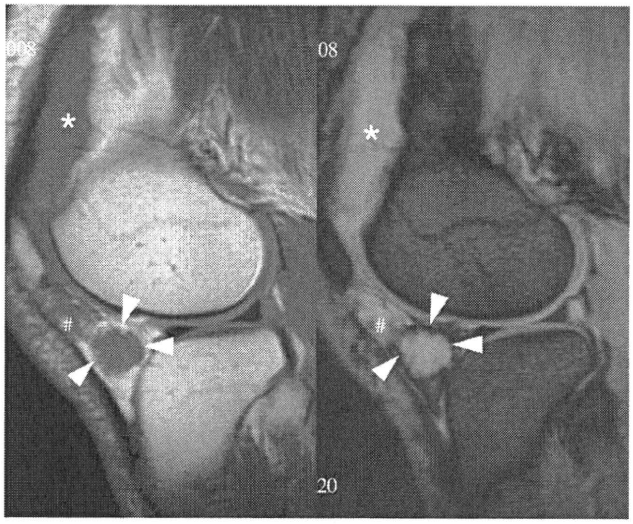

Fig. 1. Conventional T1 and T2 images (Case 1). MR images from the primary hospital show a T1 low-intensity and T2 high-intensity lesion within the infrapatellar fat pad (arrow heads). The intensity of this lesion on both T1 and T2 images is almost identical to the corresponding intensity of a nearby joint effusion (*). Adjacent to the lesion, possible satellite lesion (#) with rather obscure border was found. [MRI: Magnetom Impact 1.0 Tesla (Siemens, Berlin, Germany), T1: TR/TE = 600/15, T2* TR/TE = 660/18, FA = 20, FOV = 130 × 130 mm,Slice thichness = 3 mm].

3. Case 2

A 60 year-old man with a 10-year history of discomfort in his right knee with no apparent ADL disturbance had a sudden onset of acute knee pain that brought him to a nearby orthopaedic hospital. A joint puncture produced 100 ml of blood. The next day he again felt joint distension and a new puncture produced 70 ml of blood. He then was referred to our hospital for diagnosis and treatment.

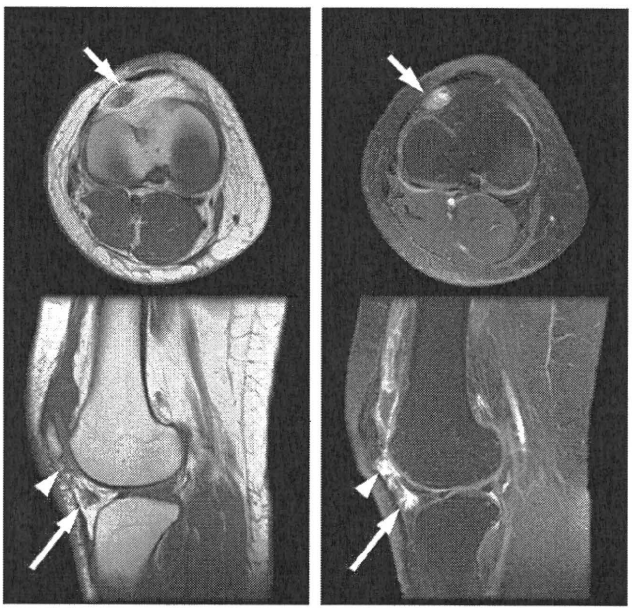

Fig. 2. Gd-enhanced images (Case 1). Prior to Gd enhancement (left column), a heterogeneously low-intensity lesion is identified on both axial and sagittal images (indicated by arrows) within the lateral area of the infrapatellar fat pad. A portion of the lesion adjacent to the inferior pole of the patella is obscured (arrowhead). Gd enhancement with fat saturation clearly depicts the extent of the tumorous lesion as homogenous enhancement with low spots throughout the lesion (right column). [MRI: Signa 1.5 T (GE Medical Systems, Milwaukee, WI), $T1^{pre}$: TR/TE = 300/9.0, $T1^{post}$: TR/TE = 500/20, FOV = 160 × 160 mm, Slice thickness = 5 mm, 10 ml of Gadopentetate dimeglumine (Magnevist, Bayer) was intravenously administered].

X-ray examination was normal, and MRI examination, including Gd enhancement, identified an intra-joint tumorous lesion (Fig. 4). Arthroscopy identified a haemangioma adjacent to the quadriceps tendon, and total excision was performed until the quadriceps tendon was totally exposed as was the same for case 1. Histological examination confirmed a diagnosis of cavernous haemangioma. No sign of recurrence was observed 2 years after surgery.

4. Discussion

Synovial haemangioma mostly involves the knee joints [6] and often arises in anterior compartment [7]. It is a relatively rare, benign condition with around 200 cases reported in the English literature. Moon et al. reported approximately 75% of patients were symptomatic prior to age 16 [8] and most of reported cases were with ages less than 30 [1–3,5,7,9–11]. But some cases were in their forties [6,11] and our case 2 appeared to be the oldest. Diagnostic delay was the specific feature of this condition [12] and in some instances it reached more than 20 years (10, case 1). Haemarthrosis is one of the commonest symptoms but not always necessary [6].

Published studies have identified the following as characteristic MRI features of synovial haemangioma: homogenous low- to iso-intensity on T1 sequence; and heterogeneous high intensity with low-intensity septa or spots within the lesion on T2 sequence (or homogenously high intensity in some instances) [3,8–15]. In addition, Llauger et al. specifically identified the following as important characteristic T2 features of synovial haemangioma: 1) lobulated configuration; 2) well-defined margins; 3) signal intensity brighter than fat; and 4) low-signal punctuate or linear structures throughout the lesion [16].

Although the above findings have diagnostic value, a variety of other intraarticular masses exhibit features similar to haemangiomas on conventional T1 and T2 sequences, including cystic synovial hyperplasia, synovial sarcoma, fibroma of the tendon sheath, leiomyioma, GCT of the tendon sheath, Schwannoma, synovial chondromatosis, and vascular malformation [3,14,17–24]. Even ganglia, which are the most common intra-knee abnormality, can mimic haemangioma because not only do they exhibit low intensity on T1 and high intensity on T2 but also most have a multiloculated/septated form that could mimic low-signal punctate or linear structures throughout the lesion [14]. Localized nodular synovitis (LNS) is to be differentiated because it shows a variety of MRI features and might mimic synovial haemangioma, though hyperintense signal on T1 seen in relatively high percentage of LNS would be of help [25]. Gd enhancement offers promise in differentiating among many of these entities. Characteristic features of Gd-enhanced images of haemangioma include inhomogenous enhancement throughout the lesion, as observed in our cases and other reported cases [3,13,26], whereas cystic synovial hyperplasia, fibroma of the tendon sheath, leiomyoma, and ganglia are enhanced only in peripheral areas or along their rims [3,14,18,20,21]. GCT of the tendon sheath, on the other hand, reportedly shows homogeneous enhancement [22]. Gd enhancement would be of help in monitoring the lesion postoperatively because it could detect the extent of the lesion clearly.

Even after Gd enhancement, differentiating between synovial sarcoma and haemangioma is difficult, especially as only a few cases of each disease have published descriptions of their Gd-enhanced imaging features [17]. The characteristic MR features of synovial haemangioma—low intensity to iso-intensity on T1, high intensity on T2, and heterogeneously high enhancement on Gd enhancement—also coincide with the characteristic MR features of malignant lesions, including intraarticular synovial sarcoma, except that most malignant lesions arise extra-articularly [27]. Although a lengthy clinical history and haemarthrosis, as occurred in our two cases, provide clinical information that can help distinguish haemangioma from malignant conditions, we have to be very careful to accurately differentiate between these two conditions.

Please cite this article as: Sasho T, et al, Two cases of synovial haemangioma of the knee joint: Gd-enhanced image features on MRI and arthroscopic excision, Knee (2010), doi:10.1016/j.knee.2010.10.004

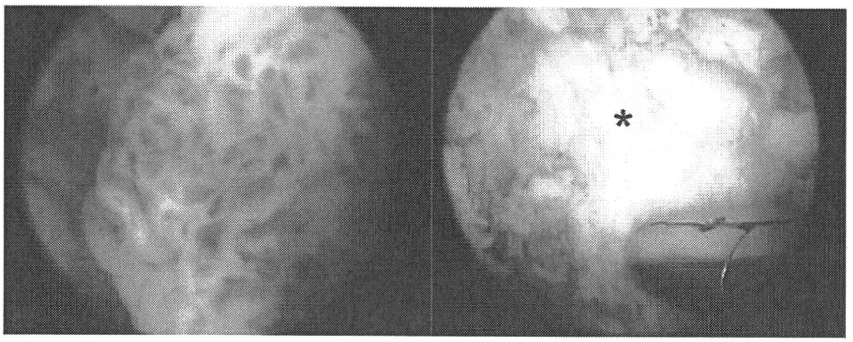

Fig. 3. Arthroscopic excision of the tumorous lesion (Case 1). This photograph shows a lesion with a strawberry-like appearance indicative of synovial haemangioma within the infrapatellar fat pad (left). The lesion was totally excised until patella tendon (*) was clearly visible (right).

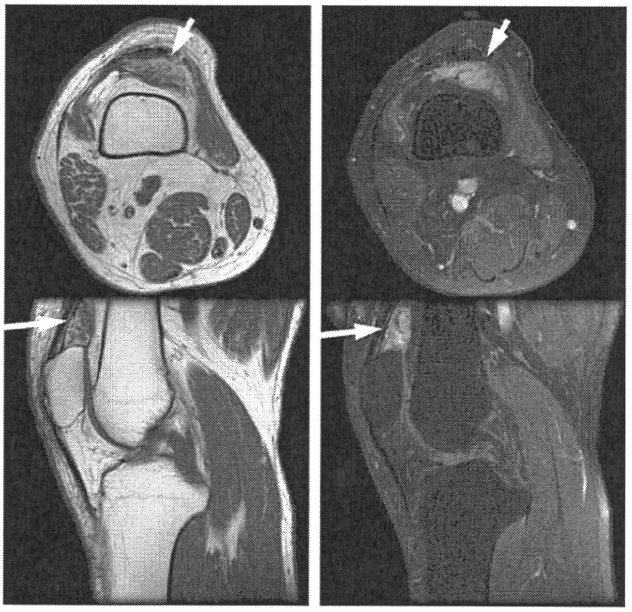

Fig. 4. Gd-enhanced images (Case 2). Prior to Gd enhancement (left column), a heterogeneously low-intensity lesion both on axial and sagittal images is identified (indicated by arrows) just behind the quadriceps tendon. Gd enhancement with fat saturation clearly depicts the extent of the tumorous lesion as homogenous enhancement with low spots and septum (right column).

5. Conclusion

Low intensity to iso-intensity on T1, high intensity on T2, and heterogeneously high intensity on Gd enhancement are characteristic MR features of synovial haemangioma of the knee joint. Gd-enhanced images are helpful in distinguishing haemangioma from other intraarticular tumorous lesions, but MR images alone cannot distinguish between synovial haemangioma and synovial sarcoma.

6. Conflict of interest

None.

Acknowledgments

This study was funded by the Comprehensive Research on Aging and Health, Health and Labor Sciences Research Grants of Japan.

References

[1] Akgun I, Kesmezacar H, Ogut T, Dervisoglu S. Intra-articular hemangioma of the knee. Arthroscopy 2003;19:1–8.
[2] Price NJ, Cundy PJ. Synovial hemangioma of the knee. J Pediatr Orthop 1997;17:74–7.
[3] De Filippo M, Rovani C, Sudberry JJ, Rossi F, Pogliacomi F, Zompatori M. Magnetic resonance imaging comparison of intra-articular cavernous synovial hemangioma and cystic synovial hyperplasia of the knee. Acta Radiol 2006;47:581–4.
[4] Barakat MJ, Hirehal K, Hopkins JR, Gosal HS. Synovial hemangioma of the knee. J Knee Surg 2007;20:296–8.
[5] Holzapfel BM, Geitner U, Diebold J, Glaser C, Jansson V, Durr HR. Synovial hemangioma of the knee joint with cystic invasion of the femur: a case report and review of the literature. Arch Orthop Trauma Surg 2008;129:143–8.
[6] Devaney K, Vinh TN, Sweet DE. Synovial hemangioma: a report of 20 cases with differential diagnostic considerations. Hum Pathol 1993;24:737–45.
[7] Helpert C, Davis AM, Evans N, Grimer RJ. Differential diagnosis of tumors and tumor-like lesions of the infrapatellar (Hoffa's) fat pad: pictorial review with an emphasis on MRI imaging. Eur Radiol 2004;14:2337–46.
[8] Moon NF. Synovial hemangioma of the knee joint. Clin Orthop Relat Res 1973;90: 183–90.
[9] Sheldon PJ, Forrester DM, Learch TJ. Imaging of intraarticular masses. Radiographics 2005;25:105–19.
[10] Okahashi K, Sugimoto K, Iwai M, Tanaka M, Fujisawa Y, Takakura Y. Intra-articular synovial hemangioma; a rare cause of knee pain and swelling. Arch Orthop Trauma Surg 2004;124:571–3.
[11] Greenspan A, Azouz EM, Matthews J, Decarie JC. Synovial hemangioma: imaging features in eight histologically proven cases, review of the literature, and different diagnosis. Skeletal Radiol 1995;24:583–90.
[12] Cotton A, Flipo RM, Herbaux B, Gougeon F, Lecomte-Houcke M, Chastanet P. Synovial haemangioma of the knee: a frequently misdiagnosed lesion. Skeletal Radiol 1995;24:257–61.
[13] Greenspan A, McGahan JP, Vogelsang P, Szabo RM. Imaging strategies in the evaluation of soft-tissue hemangiomas of the extremities: correlation of the findings of plain radiography, angiography, CT, MRI, and ultrasonography in 12 histologically proven cases. Skeletal Radiol 1992;21:11–8.
[14] Kim SJ, Cho SH, Ko DH. Arthroscopic excision of synovial hemangioma of the hip joint. J Orthop Sci 2008;13:387–9.
[15] Tzurbakis M, Mouzopoulos G, Morakis E, Nikolaras G, Georgilas I. Intra-articular knee haemangioma originating from the anterior cruciate ligament: a case report. J Med Case Rep 2008;2:254.
[16] Llauger J, Monill JM, Palmer J, Clotet M. Synovial hemangioma of the knee: MRI findings in two cases. Skeletal Radiol 1995;24:579–81.
[17] Bui-Mansfield LT, O'Brien SD. Magnetic resonance appearance of intra-articular synovial sarcoma: case reports and review of the literature. J Comput Assist Tomogr 2008;32:640–4.
[18] Takakubo Y, Fukushima S, Asano T, Yamakawa M. Case reports: intraarticular fibroma of the tendon sheath in the knee. Clin Orthop Relat Res 2005;439:280–5.
[19] Aynaci O, Kerimoglu S, Ozturk C, Saracoglu M, Yildiz K. Intraarticular fibroma of the tendon sheath arising from the infrapatellar fat pad in the knee joint. Arch Orthop Trauma Surg 2009;129:291–4.
[20] Pinar H, Ozkan M, Ozaksoy D, Pabuccuoglu U, Akseki D, Karaoglan O. Intraarticular fibroma of the tendon sheath of the knee. Arthroscopy 1995;11:608–11.
[21] Shimidt-Rohlfing B, Tietze L, Siebert CH, Staatz G. Deep soft-tissue leioma of the popliteal fossa in a 14-year old girl. Arch Orthop Trauma Surg 2001;121:604–6.
[22] Sheppard DG, Kim ED, Yasko AW, Ayala A. Giant-cell tumor of the tendon sheath arising from the posterior cruciate ligament of the knee: a case report and review of the literature. Clin Imaging 1998;22:428–30.
[23] Fisher B, Munaretto F, Fritschy D, Peter RE. An unusual arthroscopic discovery: an intraarticular Schwannoma of the knee. Arthroscopy 1994;10:113–7.
[24] Comert RB, Aydingoz U, Atay OA, Gedikoglu G, Doral MN. Vascular malformation in the infrapatellar (Hoffa's) fat pad. Knee 2004;11:137–40.
[25] Huang GS, Lee CH, Chan WP, Yu JS, Resnick D. Localized nodular synovitis of the knee: MR imaging appearance and clinical correlates in 21 patients. AJR 2003;181: 539–43.
[26] Waldt S, Rechl H, Rummeny E, Woertler K. Imaging of benign and malignant soft-tissue masses of the foot. Eur Radiol 2003;13:1125–36.
[27] Tuncbilek N, Karakas HM, Okten OO. Dynamic contrast enhanced MRI in the differential diagnosis of soft tissue tumors. Eur J Radiol 2005;53:500–5.

Please cite this article as: Sasho T, et al, Two cases of synovial haemangioma of the knee joint: Gd-enhanced image features on MRI and arthroscopic excision, Knee (2010), doi:10.1016/j.knee.2010.10.004

Articular Cartilage Repair Using an Intra-Articular Magnet and Synovium-Derived Cells

Junji Hori,[1] Masataka Deie,[2] Takaaki Kobayashi,[1] Yuji Yasunaga,[3] Seiichi Kawamata,[4] Mitsuo Ochi[1]

[1]Department of Orthopaedic Surgery, Graduate School of Biomedical Sciences, Hiroshima University, Hiroshima, Japan, [2]Department of Physical Therapy and Occupational Therapy Sciences, Graduate School of Health Sciences, Hiroshima University, Hiroshima, Japan, [3]Department of Artificial Joints and Biomaterials, Graduate School of Biomedical Sciences, Hiroshima University, Hiroshima, Japan, [4]Department of Anatomy and Histology, Graduate School of Health Sciences, Hiroshima University, Hiroshima, Japan

Received 24 April 2010; accepted 23 August 2010
Published online 4 November 2010 in Wiley Online Library (wileyonlinelibrary.com). DOI 10.1002/jor.21267

ABSTRACT: The purpose of this study was to investigate the chondrogenic potential of magnetically labeled synovium-derived cells (M-SDCs) and examine whether M-SDCs could repair the articular cartilage using an intra-articular magnet after delivery to the lesion. Synovium-derived cells (SDCs) were cultured from the synovium of a rat knee, and were magnetically labeled with ferumoxides. M-SDCs were examined with a transmission electron microscope. A pellet culture system was used to evaluate the chondrogenic potential of M-SDCs in a magnetic field. In a rat model, allogeneic M-SDCs were injected into the knee after we made an osteochondral defect on the patellar groove and implanted an intra-articular magnet at the bottom of the defect. We histologically examined the defects at 48 h, 4 weeks, 8 weeks, and 12 weeks after treatment. Electron microscopy showed the transfection of ferumoxides into SDCs. The pellet cultures revealed the chondrogenic potential of M-SDCs in a magnetic field. M-SDCs accumulated in the osteochondral defect at 48 h after treatment, and we confirmed the regeneration of the articular cartilage at 4 weeks, 8 weeks, and 12 weeks after treatment using an intra-articular magnet. We demonstrated that articular cartilage defects could be repaired using an intra-articular magnet and M-SDCs. We believe that this system will be useful to repair human articular cartilage defects. © 2010 Orthopaedic Research Society. Published by Wiley Periodicals, Inc. J Orthop Res 29:531–538, 2011

Keywords: cell delivery system; magnet; synovium; intra-articular injection; cartilage repair

Articular cartilage is well known to have very limited self-healing potential. There are many procedures, including drilling, abrasion, microfracture, and distraction, for repairing the articular cartilage.[1–7] However, the defects are repaired by fibrous tissues during those procedures,[6,8] and a routine procedure for articular cartilage defect repair has not yet been established.

Currently, engineered cartilage tissues are in widespread clinical use, and good clinical results have been achieved with these tissues.[9,10] However, this procedure requires the harvesting of a small amount of cartilage tissues from the patient prior to cartilage transplantation. It is therefore necessary to implement a less-invasive procedure.

Recently, synovium-derived cells (SDCs) have been found to have a high potential for both proliferation and differentiation.[11–15] Synovial tissues are easy to harvest and may be collected from any joint without damaging the articular cartilage. We therefore evaluated the method of transplanting SDCs for repairing articular cartilage defects.

Previous studies have suggested that intra-articular injected mesenchymal stem cells (MSCs) mobilize to the injured tissues.[16] This transplantation was less invasive, but was inefficient because the injected cells spread throughout the joint space. Consequently, we created an intra-articular magnet which had a strong magnetic force, for efficient transplantation. The delivered cells were magnetically labeled with ferumoxides, which is approved by the United States Food and Drug Administration (FDA) as a magnetic resonance contrast agent for humans. There have been no reports thus far describing a cell delivery system using an intra-articular magnet and transplanted SDCs. The purpose of this study was to confirm the chondrogenic potential of magnetically labeled SDCs (M-SDCs), and to examine whether SDCs could be delivered to the articular cartilage defect and subsequently repair the lesion in the presence of a magnetic field caused by an intra-articular magnet.

MATERIALS AND METHODS

All procedures were performed with approval from the Guide for Animal Experimentation, Hiroshima University, and the Committee of Research Facilities for Laboratory Animal Sciences, Graduate School of Biomedical Sciences, Hiroshima University.

Cell Culture

Sprague–Dawley rats at 11 weeks of age were anesthetized using sodium pentobarbital (50 mg/kg, i.p.) and their knee joints opened via a paramedian approach. The synovium was harvested from the transitional zone between the articular cartilage and the synovial membrane at the medial femoral condyle. All synovial tissues were cultured in Dulbecco's modified Eagle medium (Invitrogen (Gibco), Paisley, Scotland) with 10% fetal bovine serum (Sigma–Aldrich, St. Louis, MO) and 1% antibiotics (penicillin, streptomycin, and fungizone; BioWhittaker, Walkersville, MD) on 60 mm dishes (Falcon; BD Biosciences, Franklin Lakes, NJ) for 4 days under a humidified atmosphere and 5% carbon dioxide at 37°C. When the synovial cells were attached to the dishes, the synovium was removed. The cells were then harvested by treatment with 0.25% trypsin and 0.02% ethylenediaminetetraacetic acid (EDTA) (2.5 g/L trypsin, 1 mmol/L EDTA solution; Nacalai Tesque, Kyoto,

Correspondence to: Junji Hori (T: 81-82-257-5233; F: 81-82-257-5234; E-mail: horijun919@yahoo.co.jp)

Japan). To expand the cells, the harvested cells were seeded as passage 1 on 100 mm dishes. The medium was changed every 3–4 days to remove nonadherent cells until the cells reached confluence. Upon reaching confluence, the cells were reseeded under the same conditions. We used passage 3 cells for the subsequent analyses, and we referred to these adherent cells as SDCs.

Magnetic Labeling of SDCs

SDCs were labeled overnight with 25 μg Fe/ml ferumoxides and 375 ng/ml poly-L-lysine (PLL) (poly-L-lysine hydrobromide; molecular weight, 388 kDa [P-1524; Sigma–Aldrich]) as a transfection agent.[17] 2.2 μl of ferumoxides stock solution (11.2 mg Fe/ml; Tanabe Seiyaku, Osaka, Japan) was added per milliliter of culture medium, without cells. PLL was then added at 3.75 μl/ml from a 0.1-mg/ml stock solution. The medium was mixed and incubated for 60 min at room temperature with occasional gentle mixing. Labeling was initiated by removal of the medium from the adherent SDCs, and medium containing the ferumoxides–PLL mixture was added. After incubation for 24 h at 37°C in the medium, SDCs were collected by trypsinization.

Experimental Procedure

Study 1: Electron Microscopic Examination

M-SDCs were centrifuged and the supernatant was discarded. Precipitated complexes were fixed with 3% glutaraldehyde in 0.1 M phosphate buffer (pH 7.4) for 2 h at 4°C and were postfixed with 1% OsO_4 in 0.1 M phosphate buffer (pH 7.4) for 2 h at 4°C, rinsed in 10% saccharose three times (20 min each), and stained en bloc in 3% aqueous uranyl acetate for 1 h at room temperature. Specimens were dehydrated in an ascending series of ethanol, were replaced with propylene oxide, and embedded in epoxy resin. Thin sections (0.1 μm) were cut, stained with 3% uranyl acetate and lead citrate, and examined with a transmission electron microscope, JEM-1200 (JEOL, Tokyo, Japan).

Study 2: Chondrogenesis In Vitro

To evaluate the effect of the magnetic force on the chondrogenic potential of M-SDCs, a modification of Johnstone's pellet culture system was performed.[18] Approximately 2×10^5 SDCs were resuspended in chondrogenic differentiation medium; DF-C (Toyobo, Osaka, Japan). DF-C consisted of 3% fatal calf serum, 5 μg/ml insulin, 5 μg/ml transferrin, 0.1 μM dexsamethazone, 5 ng/ml TGFβ-1, and 5 ng/ml BMP-2. SDCs were centrifuged to form a pellet. The pellet of SDCs remained on the bottom of 15 ml polypropylene tube. The pelleted SDCs were cultured at 37°C with 5% CO_2 in 1 ml of DF-C. As the positive control group, the pellet of nonlabeled SDCs was cultured for 21 days in DF-C with no magnetic force (nonlabeled group, $n = 6$). To assess the influence of magnetically labeling and magnetic force, the pellet from M-SDCs was cultured in DF-C under an external magnetic force (magnetic force group, $n = 6$) or with no magnetic force (nonmagnetic force group, $n = 6$). In the magnetic force group, a samarium cobalt magnet (4 mm in diameter and 1.5 mm in length; magnetic flux density: 0.2 T) was positioned on the lateral side of a 15 ml polypropylene tube.[19] The medium was changed every 3 days. After 21 days in culture, the specimens were fixed with 4% paraformaldehyde and embedded in paraffin wax. To evaluate the chondrogenic ability of the three different groups, the blocks were cut into 5 μm sections with a microtome, and were stained with toluidine blue and safranin-O/fast green.

Study 3: Transplantation In Vivo

We used skeletally immature Sprague–Dawley rats at 11 weeks of age. Their mean weight was 0.4 kg. Before surgery, the rats were anesthetized with an intraperitoneal injection of 1 ml/kg pentobarbital sodium. The patella was everted through a medial approach. We made an osteochondral defect measuring 2 mm in diameter and 1 mm depth on the articular cartilage of the patellar groove of the distal femur using a drill. A column-shaped Pt–Fe permanent magnet of 1.0 T (1 mm in diameter and 3 mm in length) or a nonmagnetic alloy (Pt–Fe, 1 mm in diameter and 3 mm in length) was implanted at the bottom of the osteochondral defect. After completion of surgery, the knees were thoroughly irrigated with normal saline. The arthrotomy was closed with interrupted 5-0 nylon sutures, and the skin was closed with continuous 5-0 nylon sutures. We randomly divided the rats ($n = 96$) into four groups. Groups A and B received a single intra-articular injection of 5.0×10^5 M-SDCs as a suspension in vehicle (phosphate-buffered saline (PBS), 50 μl) after placing the permanent magnet (group A, $n = 24$) or nonmagnetic alloy (group B, $n = 24$). Groups C and D received a single intra-articular injection of 5.0×10^5 nonlabeled SDCs as a suspension in vehicle (PBS, 50 μl) after placing the permanent magnet (group C, $n = 24$) or nonmagnetic alloy (group D, $n = 24$). All groups received injections using a microsyringe for the subcutaneous insulin infusion (29-gauge needle). We confirmed that there were no areas of leakage around the knees. After the completion of all interventions, the rats were returned to their cages and were free to exercise.

Tissue Preparation

At 48 h, 4 weeks, 8 weeks, and 12 weeks following treatment, the rats were euthanized with an overdose of pentobarbital. The condyles of the femurs were dissected and fixed in 10% buffered formalin (Sigma–Aldrich Japan, Tokyo, Japan) for 48 h. The condyles were decalcified with 0.5 M EDTA solution. The specimens were dehydrated through a graded ethanol and xylene series and were embedded in paraffin wax. The blocks were cut into 5 μm serial sections along the longitudinal plane, which included the center of the defect, using a microtome.

Delivery of M-SDCs

To evaluate the efficiency of this magnetically responsive delivery system in an articular cartilage defect model, the rats were euthanized 48 h after treatment, and osteochondral defects were histologically evaluated. The accumulation of SDCs at the target site was evaluated under Berlin blue and BrdU. The BrdU (5-bromo-2′-deoxyuridin) labeling solution (Sigma–Aldrich Japan; 50 mM) was prepared in PBS. Prior to labeling with the ferumoxides, 20 μl of the BrdU labeling solution was added to each dish at a final concentration of 100 μM, and SDCs were incubated for 24 h. After preparing the sections, anti-BrdU-Fluos antibody was used for detection of BrdU-positive cells (Roche Diagnostics, Basel, Switzerland).

Cartilage Repair In Vivo

To evaluate the cartilage repair of the osteochondral defects, the rats were euthanized at 4, 8, and 12 weeks after treatment, and osteochondral defects were histologically evaluated. The cartilage repair was evaluated by examination of sections stained with toluidine blue and safranin-O/fast green. For the

immunohistological evaluations, the sections were immersed in 0.3% H_2O_2 to block endogenous peroxidase activity. The sections were blocked with normal horse serum and incubated with anti-collagen type II (Chemicon (Millipore), Billerica, MA). The visualization reaction was performed using a 3,3′-diaminobenzidine (DAB) substrate kit (Vector Laboratories, Burlingame, CA).

The 4-, 8-, and 12-week specimens were quantified using a histological grading scale for cartilage defects as described by Wakitani et al.[20] The grading scale was based on cellular morphology (0–4 points), matrix staining (0–3 points), surface regularity (0–3 points), thickness of cartilage (0–2 points), and the integration of donor to host adjacent cartilage (0–2 points). The total scores ranged from 0 to 14 points. According to this scale, a maximum score of 14 points was possible, with a better-quality repair resulting in a lower point score. We also used the modified O'Driscoll scale to evaluate the cartilage repair of the osteochondral defects.[21,22] The grading scale was based on cellular morphology (0–4 points), matrix staining (0–3 points), surface regularity (0–3 points), structural integrity (0–2 points), thickness (0–2 points), bonding to the adjacent cartilage (0–2 points), hypocellularity (0–3 points), chondrocyte clustering (0–2 points), and freedom from degenerative changes in adjacent cartilage (0–3 points). The total scores ranged from 0 to 24 points. According to this scale, a maximum score of 24 points was possible, with a better-quality repair resulting in a higher point score.

Statistical Analysis

A two-way analysis of variance test was used to compare the histological scores among the groups. When a significant p-value was obtained, a one-way ANOVA and post hoc testing using the Bonferroni test was performed to identify any significant differences among the groups. Statistical differences were considered significant for p-values <0.05.

RESULTS

Study 1: Electron Microscopic Examination

Electron microscopy showed that black particles, which represented ferumoxides, were present in SDCs (Fig. 1). The particles were present in the lysosomes of SDCs. We confirmed ferumoxides transfection into SDCs with an electron microscopic analysis.

Study 2: Chondrogenesis In Vitro

After 21 days in culture, pellet formation was confirmed in all groups. The matrices of the nonmagnetic and magnetic force groups were stained brown due to ferumoxides transfection. The toluidine blue and safranin-O/fast green staining of the magnetic force group and nonmagnetic force group was comparable with the staining of the nonlabeled group (Fig. 2). We found the chondrogenic potential of M-SDCs in a magnetic field was equivalent to nonlabeled SDCs.

Study 3: Transplantation In Vivo

Delivery of M-SDCs

At 48 h after treatment, there were many cells stained with Berlin blue in the osteochondral defect in group A (Fig. 3a). In the other groups, there were no cells stained with Berlin blue (Fig. 3b–d). In group A, many cells were also stained with BrdU on the defect (Fig. 3e). In groups B–D, some cells were stained with BrdU (Fig. 3f–h), indicating that M-SDCs could accumulate in the osteochondral defect using an intra-articular magnet.

Cartilage Repair In Vivo

At 4 weeks after treatment, the staining of toluidine blue on osteochondral defects was poor in all groups (Fig. 4a–d). The defects were almost completely filled with fibrous tissues, which cannot be stained with toluidine blue. In group A, the defects were partially covered with the tissues containing chondrocyte-like cells stained with toluidine blue (Fig. 4a). At 8 weeks after treatment, the irregularity of the surfaces of the osteochondral defects was decreased compared to those at 4 weeks (Fig. 4e–h). In particular, the tissues stained with toluidine blue on the surfaces were abundant in group A (Fig. 4e). There were also chondrocyte-like cells containing cartilage lacuna on the defects in group A. At 12 weeks after treatment, the defects were covered with the tissue containing chondrocyte-like cells stained with toluidine blue in all groups (Fig. 4i–l). In group A, the thickness of the regenerated cartilage and the integration with the surrounding normal articular cartilage were both increased compared to the other groups (Fig. 4i).

The intensity of safranin-O/fast green and type II collagen staining in the defects increased over time in a manner similar to the toluidine blue (data not shown). At 12 weeks after treatment, the defects were stained with safranin-O/fast green in all groups (Fig. 5a–d). In particular, the regenerated cartilage had a similar

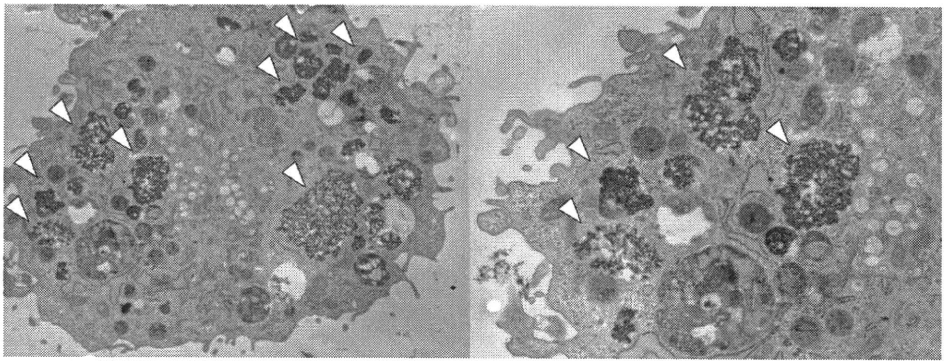

Figure 1. Electron microscopic findings of M-SDCs. The white arrowheads indicate the particles of ferumoxides in the lysosomes of the SDCs (original magnification, left ×4,000, right ×8,000).

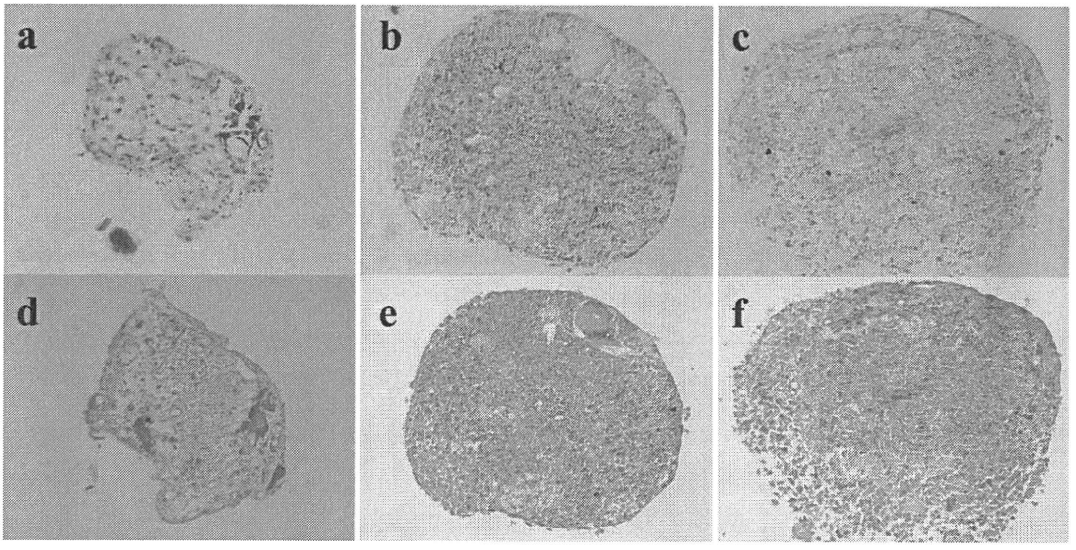

Figure 2. Microscopic findings of the pellet. The upper side indicates the results of toluidine blue staining, and the lower side represents samples stained with safranin-O/fast green (a,d, nonlabeled group; b,e, nonmagnetic force group; c,f, magnetic force group. Original magnification ×200).

staining pattern to the surrounding normal articular cartilage, with clear positive staining of the extracellular matrix around the chondrocyte-like cells on the defect in group A (Fig. 5a). The type II collagen staining in the defects were also present in all groups (Fig. 5e–h). There were thick layers of chondrocyte-like cells in the defects of group A compared with other groups (Fig. 5e).

The histological scores of the Wakitani scale were significantly lower in group A than in groups B–D at all time points after treatment, especially at 12 weeks ($p < 0.01$) (Fig. 6). The mean histological scores were 8.3 at 4 weeks, 6.0 at 8 weeks, and 4.5 at 12 weeks, in group A. The histological scores of the modified O'Driscoll scale were significantly higher in group A than in groups B–D at all time points after treatment ($p < 0.05$) (data not shown). The mean histological scores were 15.7 at 4 weeks, 17.7 at 8 weeks, and 19.3 at 12 weeks, in group A.

DISCUSSION

We have herein demonstrated that M-SDCs have a chondrogenetic potential. We also showed that our system, using an intra-articular magnet, is sufficient to deliver M-SDCs to the sites of articular cartilage defects and repair the lesions. This is the first report to transplant M-SDCs to the target site using an intra-articular magnet.

Recently, there have been many reports of transplanting MSCs to the articular cartilage defects.[23–26] The results of transplanting MSCs are satisfactory. Among the varied procedures for repairing articular cartilage defects, there are several reports regarding the intra-articular injection of MSCs. Murphy et al.[23] reported that intra-articular injection of MSCs accelerated regeneration of articular cartilage of goat knees, and Nishimori et al.[24] reported that intra-articular injection of MSCs, along with stimulation of

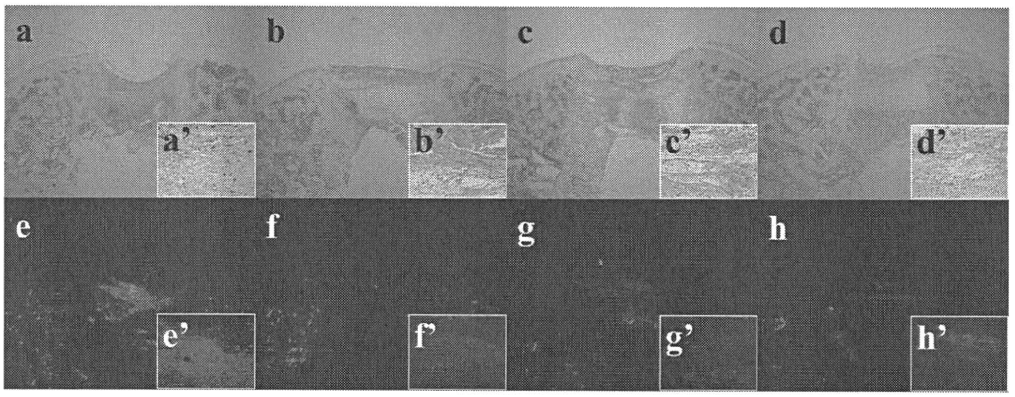

Figure 3. Microscopic findings at 48 h following treatment. The upper side represents samples stained with Berlin blue, and the lower side represents BrdU-stained samples (aa', ee', group A; bb', ff', group B; cc', gg', group C; dd', hh', group D. Groups A and B received a single intra-articular injection of 5.0×10^5 M-SDCs after placing the permanent magnet (group A) or nonmagnetic alloy (group B). Groups C and D received a single intra-articular injection of 5.0×10^5 nonlabeled SDCs after placing the permanent magnet (group C) or nonmagnetic alloy (group D). Original magnification, a–h ×40, a'–h' ×400).

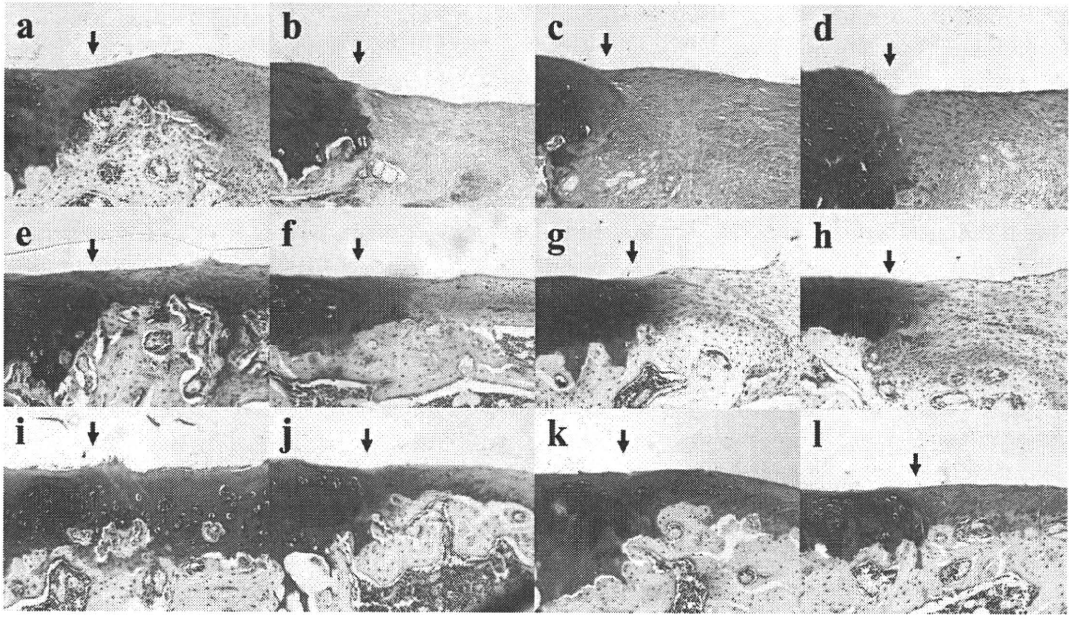

Figure 4. Microscopic findings of toluidine blue at 4 weeks (a–d), 8 weeks (e–h), and 12 weeks (i–l) following treatment. The black arrows indicate the junction between the normal articular cartilage and the artificial defect (a, e, i, group A; b, f, j, group B; c, g, k, group C; d, h, l, group D. Original magnification ×200).

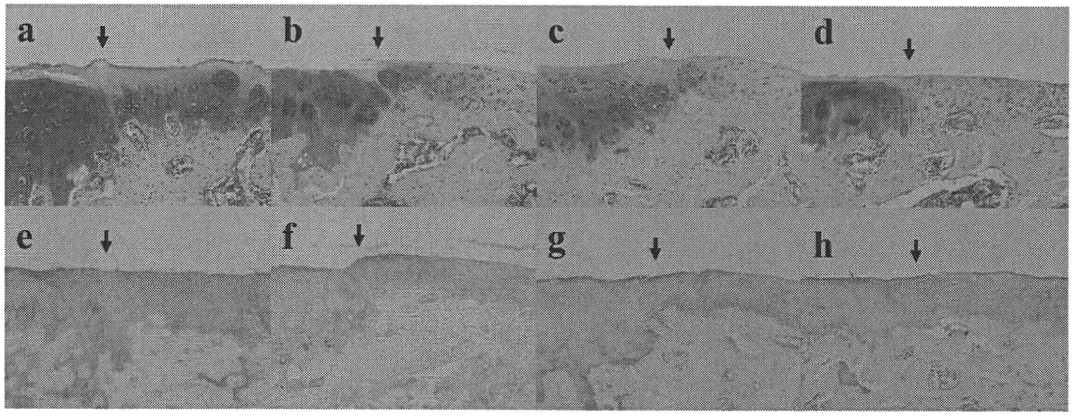

Figure 5. Microscopic findings at 12 weeks following treatment. The upper side represents samples stained with safranin-O/fast green, and the lower side represents the immunohistochemical staining for type II collagen. The black arrows indicate the junction between the normal articular cartilage and the artificial defect (a, e, group A; b, f, group B; c, g, group C; d, h, group D. Original magnification ×200).

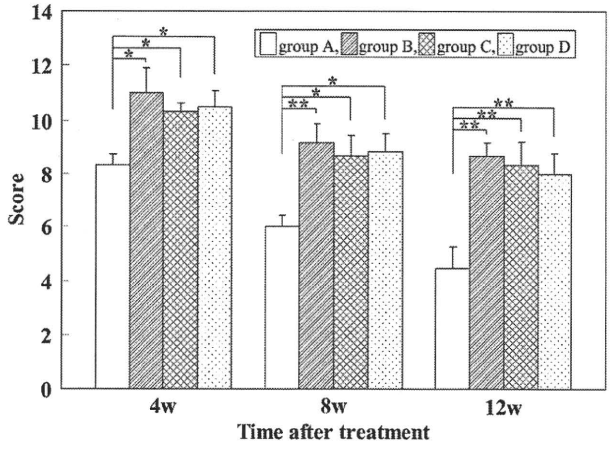

Figure 6. Histological grading scores for osteochondral defects after treatment. $n = 6$ for each group. The data are expressed as the mean ± SD (*$p < 0.05$, **$p < 0.01$). w, week(s).

bone marrow, repaired chronic osteochondral defects of rat knees. However, these procedures can cause serious complications. Agung et al.[16] reported that intra-articular injection of 1.0×10^7 MSCs generated free bodies of scar tissue in the rat knee. Therefore, we must improve the efficiency of this procedure for transplanting a small amount of MSCs to the articular cartilage defect.

Previously, we reported several drug and cell delivery systems using a magnetic force.[9,27–41] Kobayashi et al.[38] reported that an external magnetic force could deliver magnetically labeled MSCs to a desired place; in that study, the authors injected magnetically labeled MSCs into swine knees. They demonstrated an ability to control the direction of magnetically labeled MSCs using an external magnetic device for arthroscopic treatment. However, if we use the magnetic device, we must prepare

operative tools that are not affected by the magnetic fields. Moreover, when we apply this method in a clinical setting, other metals in the patient, such as heart pacers, will be a problem. Therefore, we created the cell delivery system using an intra-articular magnet that can localize the magnetic force to a small area.

Recently, it has been shown that SDCs have great proliferation and differentiation potential.[11–15] De Bari et al.[11] first reported that synovium-derived MSCs demonstrated multipotent differentiation, specifically chondrogenesis, osteogenesis, myogenesis, and adipogenesis, in vitro. Sakaguchi et al.[13] have reported that human synovium-derived MSCs had a greater proliferation and chondrogenic ability than MSCs derived from other tissues such as the bone marrow, periosteum, adipose tissue, and muscle, in vitro. Consequently, we set out to repair articular cartilage defects using SDCs and the foregoing cell delivery system.

Our study showed that a certain amount of repair occurs in the articular cartilage defects after intra-articular injection of SDCs, whether intra-articular magnets are used or not. These results proved the effectiveness of only the intra-articular injection of MSCs. However, we have confirmed an earlier and more efficient regeneration of the articular cartilage using an intra-articular magnet and M-SDCs. We herein demonstrated that this cell delivery system is both efficient and effective.

There were some surgical complications in the rat models; magnet dislocation (1 knee), infection (3 knees), anesthetic death (2 rats), and they were all excluded from the study group. In order to prevent the surgical complications especially infection, we harvested the synovium, cultured SDCs, placed the intra-articular magnets, and injected the cells into the joint using aseptic techniques. We did not evaluate whether the synovium had inflammatory cells or not when we harvested it, but if there were some inflammatory cells leading to infection in the synovium, then some signs of infection, such as the white turbidity of the medium, appeared after seeding on the dish. We excluded the cells with a suspected infection from the transplantation trials.

In clinical practice, autologous chondrocyte implantation (ACI) is a favorable method for repairing large and deep cartilage defects. ACI has demonstrated good clinical results.[9,42] However, if we use this method, we need to open the joint, and thereby increase the risk of infection. Our system using an intra-articular magnet and M-SDCs has a smaller risk of infection because we can harvest the synovium and place the magnet by means of arthroscopic surgery without the need to open the joint in the future. Additionally, we can transplant the cells to the osteochondral defect using an intra-articular injection, and therefore this system is considered to be less invasive.

There are some limitations to the current study. When we magnetically labeled SDCs, we used ferumoxides, which are approved by the United States FDA, and the safety of these compounds has been confirmed in humans. However, it is not known whether labeling with ferumoxides inhibits the chondrogenic differentiation capacity of MSCs. Kostura et al.[43] reported that ferumoxides labeling markedly inhibited MSC chondrogenesis. In contrast, Arbab et al.[44] reported that ferumoxides labeling had no inhibitory effects on chondrogenesis. In this study, we confirmed that ferumoxides did not inhibit SDC chondrogenesis in pellet culture, and we believe that magnetic labeling has no adverse effects on differentiation. Further, we used a Pt–Fe magnet for this study in vivo. This magnet is effective for collecting magnetically labeled cells because it is rustproof and permanently maintains the strong magnetic force. The Pt–Fe alloy has been used clinically in the field of dentistry, such as in the production of crowns and bridges, and the safety and durability of this alloy has been confirmed in vivo. However, if we use this magnet for humans, we must remove the magnet after repairing the cartilage, which may thus be technically difficult as well as invasive for the patient. When we apply this cell delivery system to the clinical setting, we hope to use a magnet that may be absorbed into the patient's body. This will require the engineering innovation of new magnetic materials.

Nonetheless, we concluded that this novel cell delivery system is useful for efficient and minimally invasive transplantation for cartilage repair. In the future, we expect to harvest the synovium and place the intra-articular magnet by means of arthroscopic surgery without the need to open the joint. For clinical application; however, further studies in large animals will be needed. We believe that this system is applicable for human articular cartilage defects caused by osteoarthritis or trauma. Moreover, this system may also be applied to other tissues such as the meniscus, tendon, muscle, bone, and nerve in the future.

ACKNOWLEDGMENTS

Part of this study won the Best Poster Presentation at the 24th Annual Research Meeting of the Japanese Orthopaedic Association, November 5–6, 2009. This study was supported in part by grants-in-aid to M.O. from the Japan Ministry of Education, Culture, Sports, Science and Technology (No. 21249079). No benefits in any form have been received or will be received from a commercial party related directly or indirectly to the subject of this article.

REFERENCES

1. Gobbi A, Nunag P, Malinowski K. 2005. Treatment of full thickness chondral lesions of the knee with microfracture in a group of athletes. Knee Surg Sports Traumatol Arthrosc 13:213–221.
2. Frisbie DD, Oxford J, Southwood L, et al. 2003. Early events in cartilage repair after subchondral bone microfracture. Clin Orthop 407:215–227.
3. Steadman JR, Rodkey WG, Rodrigo JJ. 2001. Microfracture: surgical technique and rehabilitation to treat chondral defects. Clin Orthop 391:362–369.

4. Johnson LL. 1986. Arthroscopic abrasion arthroplasty historical and pathologic perspective: present status. Arthroscopy 2:54–69.
5. Pridie KH. 1959. A method of resurfacing osteoarthritic joints. J Bone Joint Surg Br 41:618–619.
6. Mitchell N, Shepard N. 1976. The resurfacing of adult rabbit articular cartilage by multiple perforations through the subchondral bone. J Bone Joint Surg Am 58:230–233.
7. Deie M, Ochi M, Adachi N, et al. 2007. A new articulated distraction arthroplasty device for treatment of the osteoarthritic knee joint: a preliminary report. Arthroscopy 23:833–838.
8. Frisbie DD, Trotter GW, Powers BE, et al. 1999. Arthroscopic subchondral bone plate microfracture technique augments healing of large chondral defects in the radial carpal bone and medial femoral condyle of horses. Vet Surg 28:242–255.
9. Ochi M, Adachi N, Nobuto H, et al. 2004. Articular cartilage repair using tissue engineering technique—novel approach with minimally invasive procedure. Artif Organs 28:28–32.
10. Adachi N, Ochi M, Deie M, et al. 2006. Lateral compartment osteoarthritis of the knee after meniscectomy treated by the transplantation of tissue-engineered cartilage and osteochondral plug. Arthroscopy 22:107–112.
11. DeBari C, Dell'Accio F, Tyzanowski P, et al. 2001. Multipotent mesenchymal stem cells from adult human synovial membrane. Arthritis Rheum 44:1928–1942.
12. Nishimura K, Solchaga LA, Caplan AI, et al. 1999. Chondroprogenitor cells of synovial tissue. Arthritis Rheum 42:2631–2637.
13. Sakaguchi Y, Sekiya I, Yagishita K, et al. 2005. Comparison of human stem cells derived from various mesenchymal tissues: superiority of synovium as a cell source. Arthritis Rheum 52:2521–2529.
14. Koga H, Muneta T, Ju YJ, et al. 2007. Synovial stem cells are regionally specified according to local microenvironments after implantation for cartilage regeneration. Stem Cells 25:689–696.
15. Miyamoto A, Deie M, Yamasaki T, et al. 2007. The role of the synovium in repairing cartilage defects. Knee Surg Sports Traumatol Arthrosc 15:1083–1093.
16. Agung M, Ochi M, Yanada S, et al. 2006. Mobilization of bone marrow-derived mesenchymal stem cells into the injured tissues after intraarticular injection and their contribution to tissue regeneration. Knee Surg Sports Traumatol Arthrosc 14:1307–1314.
17. Bulte JW, Arbab AS, Douglas T, et al. 2004. Preparation of magnetically labeled cells for cell tracking by magnetic resonance imaging. Methods Enzymol 386:275–299.
18. Johnstone B, Hering TM, Caplan AI, et al. 1998. In vitro chondrogenesis of bone marrow-derived mesenchymal progenitor cells. Exp Cell Res 238:265–272.
19. Yanada S, Ochi M, Adachi N, et al. 2006. Effects of CD44 antibody- or RGDS peptide-immobilized magnetic beads on cell proliferation and chondrogenesis of mesenchymal stem cells. J Biomed Mater Res A 77:773–784.
20. Wakitani S, Goto T, Pineda SJ, et al. 1994. Mesenchymal cell-based repair of large, full-thickness defects of articular cartilage. J Bone Joint Surg Am 76:579–592.
21. O'Driscoll SW, Keeley FW, Salter RB. 1986. The chondrogenic potential of free autogenous periosteal grafts for biological resurfacing of major full-thickness defects in joint surfaces under the influence of continuous passive motion. An experimental investigation in the rabbit. J Bone Joint Surg Am 68:1017–1035.
22. Moojen DJ, Saris DB, Auw Yang KG, et al. 2002. The correlation and reproducibility of histological scoring systems in cartilage repair. Tissue Eng 8:627–634.
23. Murphy JM, Fink DJ, Hunziker EB, et al. 2003. Stem cell therapy in a caprine model of osteoarthritis. Arthritis Rheum 48:3464–3474.
24. Nishimori M, Deie M, Kanaya A, et al. 2006. Repair of chronic osteochondral defects in the rat. A bone marrow-stimulating procedure enhanced by cultured allogenic bone marrow mesenchymal stromal cells. J Bone Joint Surg Br 88:1236–1244.
25. Wakitani S, Imoto K, Yamamoto T, et al. 2002. Human autologous culture expanded bone marrow mesenchymal cell transplantation for repair of cartilage defects in osteoarthritic knees. Osteoarthritis Cartilage 10:199–206.
26. Tatebe M, Nakamura R, Kagami H, et al. 2005. Differentiation of transplanted mesenchymal stem cells in a large osteochondral defect in rabbit. Cytotherapy 7:520–530.
27. Kubo T, Sugita T, Shimose S, et al. 2000. Targeted delivery of anticancer drugs with intravenously administered magnetic liposomes in osteosarcoma-bearing hamsters. Int J Oncol 17:309–315.
28. Kubo T, Sugita T, Shimose S, et al. 2001. Targeted systemic chemotherapy using magnetic liposomes with incorporated adriamycin for osteosarcoma in hamsters. Int J Oncol 18:121–125.
29. Hirao K, Sugita T, Kubo T, et al. 2003. Targeted gene delivery to human osteosarcoma cells with magnetic cationic liposomes under a magnetic field. Int J Oncol 22:1065–1071.
30. Matsuo T, Sugita T, Kubo T, et al. 2003. Injectable magnetic liposomes as a novel carrier of recombinant human BMP-2 for bone formation in a rat bone-defect model. J Biomed Mater Res A 66:747–754.
31. Nobuto H, Sugita T, Kubo T, et al. 2004. Evaluation of systemic chemotherapy with magnetic liposomal doxorubicin and a dipole external electromagnet. Int J Cancer 109:627–635.
32. Hamasaki T, Tanaka N, Ishida O, et al. 2005. Characterization of labeled neural progenitor cells for magnetic targeting. Neuroreport 16:1641–1645.
33. Nakashima Y, Deie M, Yanada S, et al. 2005. Magnetically labeled human natural killer cells, accumulated in vitro by an external magnetic force, are effective against HOS osteosarcoma cells. Int J Oncol 27:965–971.
34. Tanaka H, Sugita T, Yasunaga Y, et al. 2005. Efficiency of magnetic liposomal transforming growth factor-beta 1 in the repair of articular cartilage defects in a rabbit model. J Biomed Mater Res A 73:255–263.
35. Nishida K, Tanaka N, Nakanishi K, et al. 2006. Magnetic targeting of bone marrow stromal cells into spinal cord: through cerebrospinal fluid. Neuroreport 17:1269–1272.
36. Kawamata S. 2006. Effects of CD44 antibody- or RGDS peptide-immobilized magnetic beads on cell proliferation and chondrogenesis of mesenchymal stem cells. J Biomed Mater Res A 77:773–784.
37. Hamasaki T, Tanaka N, Kamei N, et al. 2007. Magnetically labeled neural progenitor cells, which are localized by magnetic force, promote axon growth in organotypic cocultures. Spine 32:2300–2305.
38. Kobayashi T, Ochi M, Yanada S, et al. 2008. A novel cell delivery system using magnetically labeled mesenchymal stem cells and an external magnetic device for clinical cartilage repair. Arthroscopy 24:69–76.
39. Sugioka T, Ochi M, Yasunaga Y, et al. 2008. Accumulation of magnetically labeled rat mesenchymal stem cells using an external magnetic force, and their potential for bone regeneration. J Biomed Mater Res A 85:597–604.
40. Kobayashi T, Ochi M, Yanada S, et al. 2009. Augmentation of degenerated human cartilage in vitro using magnetically labeled mesenchymal stem cells and an external magnetic device. Arthroscopy 25:1435–1441.

41. Motoyama M, Deie M, Kanaya A, et al. 2010. In vitro cartilage formation using TGF–immobilized magnetic beads and mesenchymal stem cell-magnetic bead complexes under magnetic field conditions. J Biomed Mater Res A 92:196–204.
42. Ochi M, Uchio Y, Kawasaki K, et al. 2002. Transplantation of cartilage-like tissue made by tissue engineering in the treatment of cartilage defects of the knee. J Bone Joint Surg Br 84:571–578.
43. Kostura L, Kraitchman DL, Mackay AM, et al. 2004. Feridex labeling of mesenchymal stem cells inhibits chondrogenesis but not adipogenesis or osteogenesis. NMR Biomed 17:513–517.
44. Arbab AS, Yocum GT, Rad AM, et al. 2005. Labeling of cells with ferumoxides-protamine sulfate complexes does not inhibit function or differentiation capacity of hematopoietic or mesenchymal stem cells. NMR Biomed 18:553–559.

原著論文

Journal of Joint Surgery Vol.30 No.5, 2011

T2マッピングによる関節軟骨の変性の評価 ―病理組織所見との対比―

岩間祐基　久保晴司　藤井正彦　後藤　一　黒田良祐　黒坂昌弘　杉村和朗

はじめに

MRIはコントラスト分解能に優れ，3T(テスラ)の超高磁場装置の導入やさまざまな撮像法の開発が進んだことにより，非侵襲的に関節軟骨を詳細に評価できるようになった[1]。なかでもT2マッピングは，関節軟骨のコラーゲン配列の破綻や，それに伴う水分含有量の増加を鋭敏に評価できる撮像法であり，関節軟骨変性を従来の形態的評価よりも早期の段階で，T2値の変化という定量的な形で評価することが可能である[2),3)]。しかし，関節軟骨変性における病理組織学的な変化が，画像所見にどのように反映するかについては，これまでに死体膝や動物実験のモデルを用いた報告はみられるが[4),5)]，実際の生体において病理像と画像所見を詳細に対比した報告は，著者らが検索した範囲では認められない。今回の研究の目的は，変形性膝関節症で人工関節置換術を予定している患者を対象に，術前MRI検査におけるT2マッピングを用いた関節軟骨の画像所見が，摘出された関節軟骨の病理組織所見をどの程度正確に反映しているかを定量的に評価することである。

Key words
MRI T2マッピング(MRI T2 mapping)
関節軟骨(articular cartilage)
変性(degeneration)
サフラニンO染色(Safranin O staining)

対象ならびに方法

対象は内側型の変形性膝関節症に対し，人工関節全置換術が施行された10名10膝(女性9例，男性1例，年齢は58～78歳，平均71.1歳)。

使用機器はPhilips社製Achieva 3T，使用コイルは8チャンネルSENSE 膝コイル，撮像条件はFOV=150×150mm，マトリックス512×512，スライス厚3mmにて，膝関節MRIを撮像した。

撮像法は，脂肪抑制プロトン密度強調像(TR/TE=3,300/10)の矢状断像，脂肪抑制T2強調像(TR/TE=3,300/90)の矢状断像，冠状断像，およびダブルエコー法によるT2マッピング(TR/dual TE=3,300/30，90)の矢状断像を作成した。

MRIと組織所見を対比するために，関節軟骨が比較的保たれている外顆荷重面において，MRIとできるだけ同じ断面で関節軟骨の組織標本を作成した。切除標本に対しサフラニンO染色を行い，関節軟骨の層構造の不明瞭化や軟骨

Evaluation of articular cartilage using T2 mapping
―Comparison with pathological findings―

0286-5394/11/¥400/論文/JCOPY

Y. Iwama, M. Fujii, H Goto, K. Sugimura：神戸大学大学院医学研究科放射線医学分野
S. Kubo, R. Kuroda, M. Kurosaka：神戸大学大学院医学研究科整形外科学

細胞の消失，軟骨基質の減少の程度などを視覚的に評価した。

視覚的な検討としては，T2強調像における信号強度の違いや軟骨の厚さから，正常に近い部位から変性が進行した部位まで，各症例で任意に5つの関心領域ROIを設定し，T2強調像およびPD強調像での信号強度を測定した。定量的な検討としては，同じ位置にROIを設定してT2マッピング像において関節軟骨のT2値を測定した。

病理組織像は，サフラニンO染色における染色性の程度を，正常群，正常と比べ70～30%程度の染色性を示すものを中等度変性群，正常と比べ30%以下の染色性を示すものを高度変性群の3段階に分類したうえで，MRIでROIを設定した部位にできできるだけ近い部位において，サフラニンO染色おける染色性(軟骨変性)の程度と，各ROIにおける信号強度およびT2値と比較検討した。

統計学的検討としては多重検定を用い，信号強度と組織所見，T2値と組織所見との関係を比較検討した(群間の有意差を5%水準にて検定)。

結果

● 信号強度と組織所見

関節軟骨は，脂肪抑制プロトン密度強調像ではほぼ均一な高信号を示す構造として描出され，脂肪抑制T2強調像では深部は低信号で表面に近づくにつれて高信号となる層構造を示した**(図1)**。統計学的な検討では，脂肪抑制PD強調

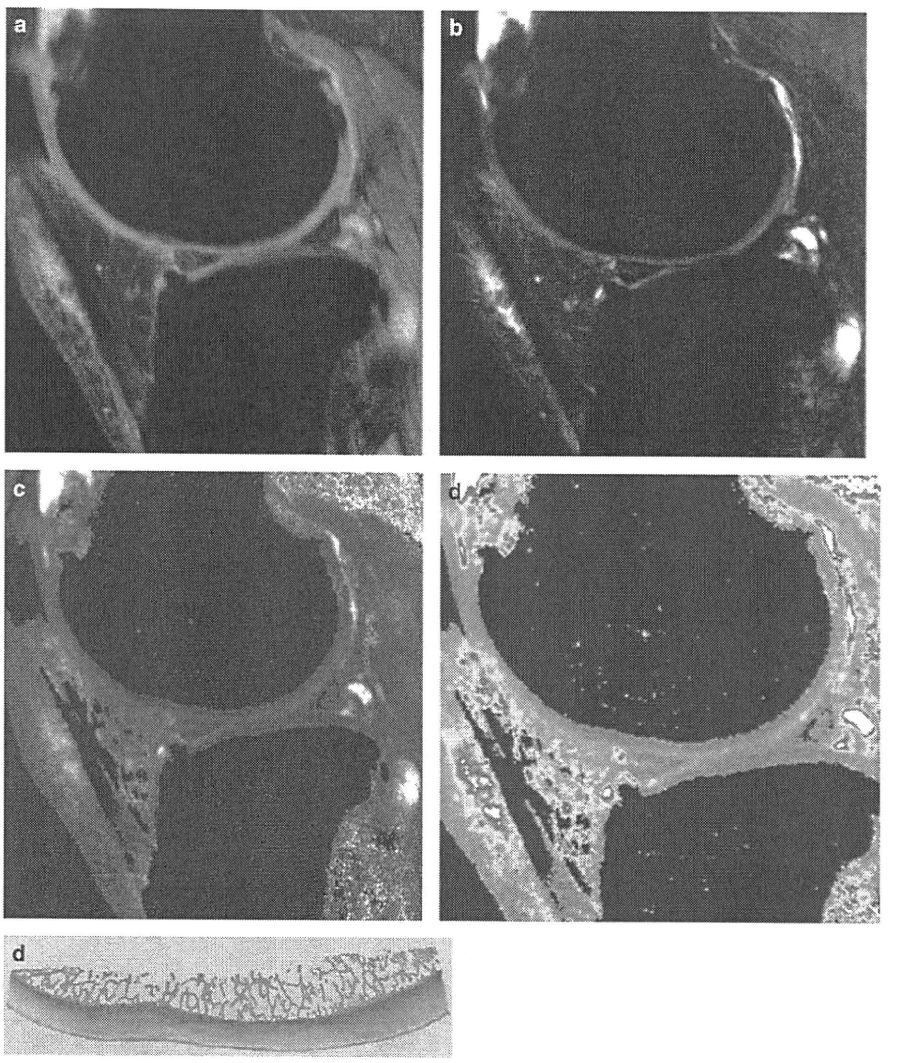

図1 60歳代，女性
a：脂肪抑制プロトン強調像。関節軟骨は厚さ数mmの層状の構造として描出されている。
b：脂肪抑制T2強調像。関節液とのコントラストは良好だが，関節軟骨の性状の評価はやや難しい。
c：T2マッピング。
d：T2マッピング(カラー)。関節軟骨は均一な層構造として描出されている(黄緑色)。
e：組織所見(サフラニンO染色)。関節軟骨は均一な層構造を示し，染色性も良好である。

像では組織所見の3群間のとの間でいずれも有意な相関は認められなかった(**図2**)。これに対して脂肪抑制T2強調像では，高度変性群は中等度変性および正常群に対して，信号強度の有意な上昇が認められた($p<0.05$)(**図3**)。

● T2値と組織所見

T2値と組織所見との比較でも，高度変性群は中等度変性群および正常群に対して，T2値の有意な延長が認められた($p<0.05$)(**図4**)。

考察

変形性膝関節症は，中高年の膝関節痛の原因として最も高頻度にみられる疾患であり，人口の高齢化により今後さらに頻度が増すと予想される。変形性膝関節症の発症には，種々の因子が関与していると思われるが，関節軟骨に対する機械的ストレスが最も大きな因子であることは確実である。しかし，機械的ストレスによって生じる関節軟骨の変性が，どのような機序で変形性膝関節症へと進展していくかについては，いまだ完全には解明されていない。

図2 脂肪抑制PD強調像の信号強度と染色性

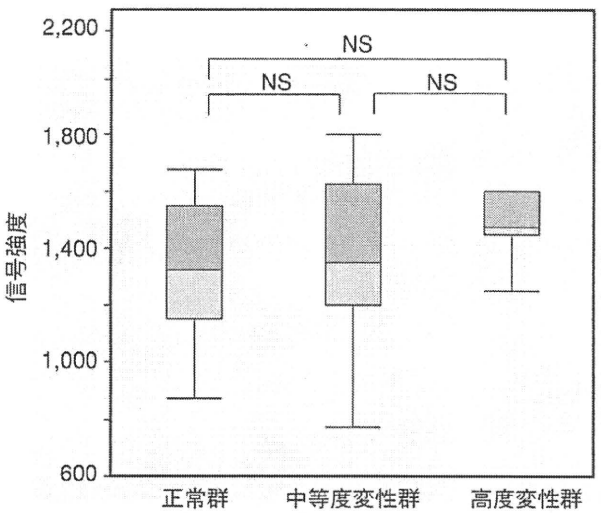

図3 脂肪抑制T2強調像の信号強度と染色性

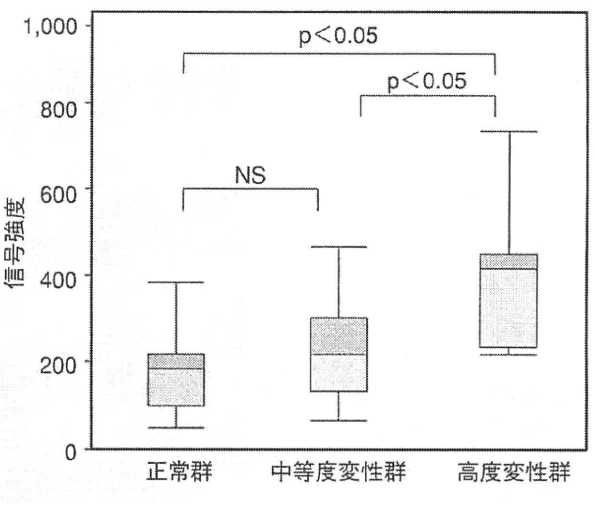

図4 T2値と染色性